Electronic Supplementary Material (ESI) for Environmental Science: Nano.

Supporting information

Sulfur containing nitrogen-rich robust hierarchically porous organic polymer for adsorptive removal of mercury: experimental and theoretical insights

Avik Chowdhury,[†,a] Sabuj Kanti Das,[†,a] Saptarsi Mondal,[b,c] Santu Ruidas,[a] Debabrata Chakraborty,[a] Sauvik Chatterjee,[a] Manas K Bhunia,[d] Debraj Chandra,[d] Michikazu Hara[e] and Asim Bhaumik*[,a]

[a]*School of Materials Sciences, Indian Association for the Cultivation of Science, 2A & 2B Raja S. C. Mullick Road, Jadavpur, Kolkata 700032, India*

[b]*Center for Molecular Spectroscopy and Dynamics, Institute of Basic Science (IBS), Seoul 02841, Republic of Korea*

[c]*Department of Chemistry, Korea University, Seoul 02841, Republic of Korea*

[d]*World Research Hub Initiative (WRHI), Institute of Innovative Research, Tokyo Institute of Technology, Midori-ku, Yokohama 226-8503, Japan*

[e]*Laboratory for Materials and Stuctures, Institute of Innovative Research, Tokyo Institute of Technology, Midori-ku, Yokohama 226-8503, Japan*

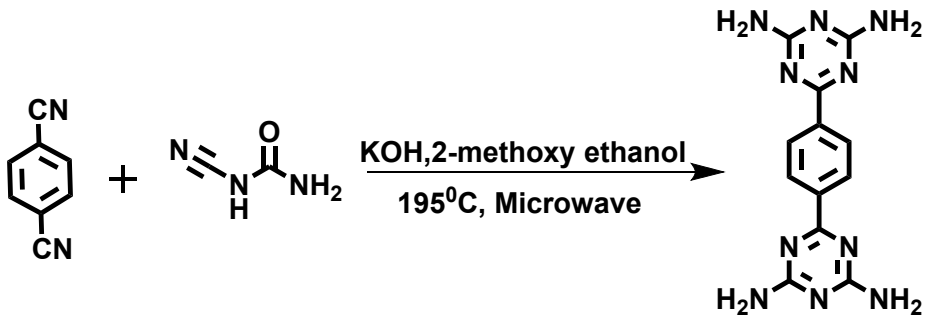

Scheme S1: Synthesis of 6,6'-(1,4-phenylene)bis(1,3,5-triazine-2,4-diamine).

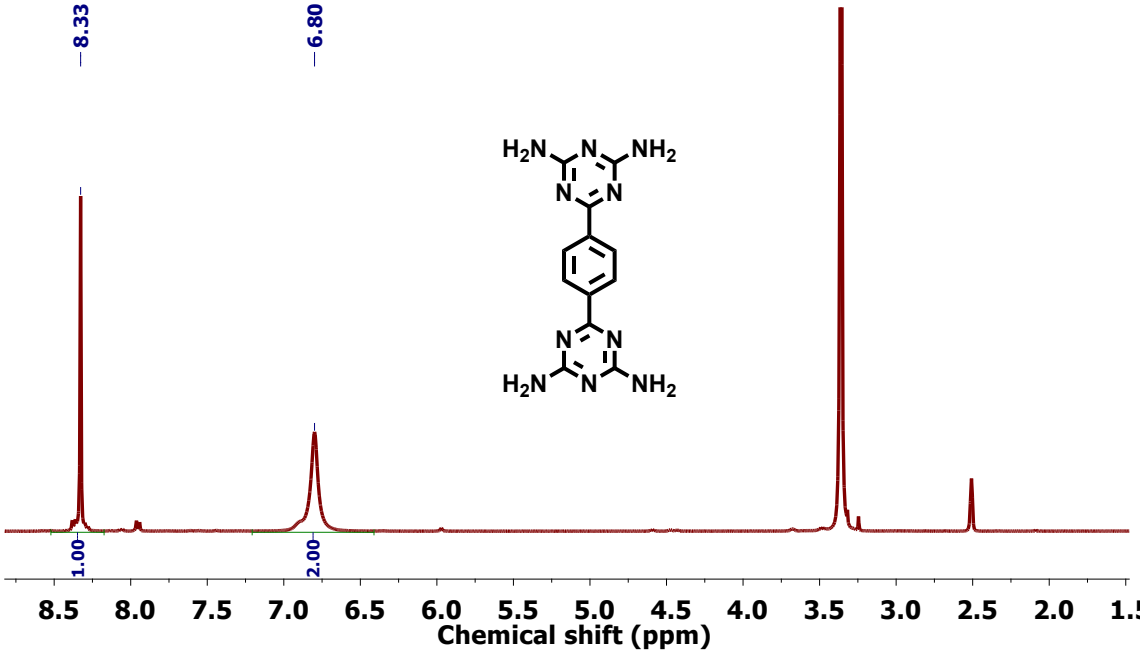

Figure S1: ^{1}H NMR of 6,6'-(1,4-phenylene)bis(1,3,5-triazine-2,4-diamine).

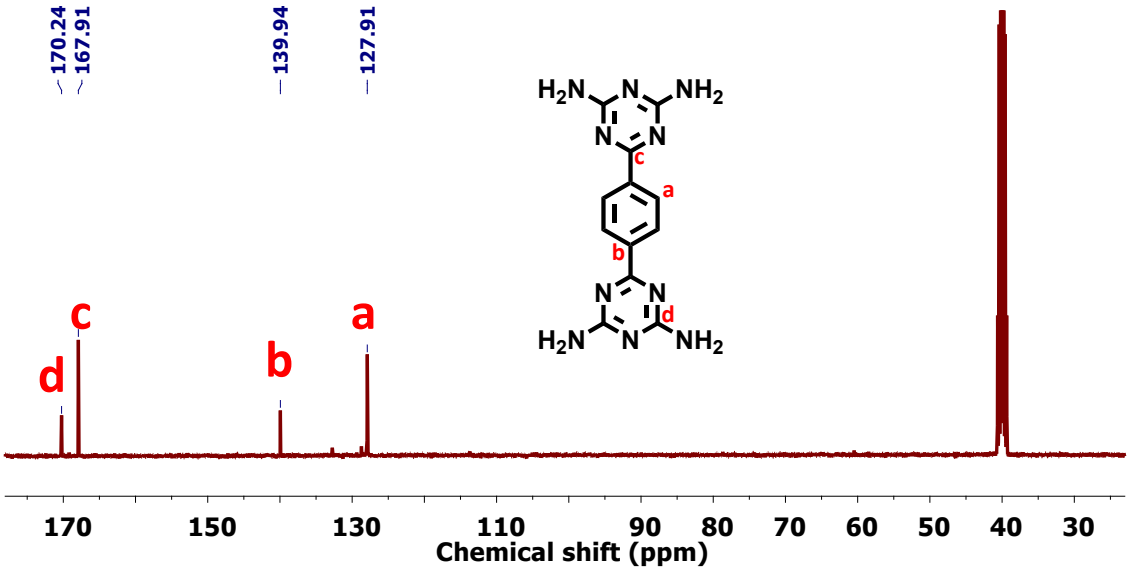

Figure S2: ^{13}C NMR of 6,6'-(1,4-phenylene)bis(1,3,5-triazine-2,4-diamine).

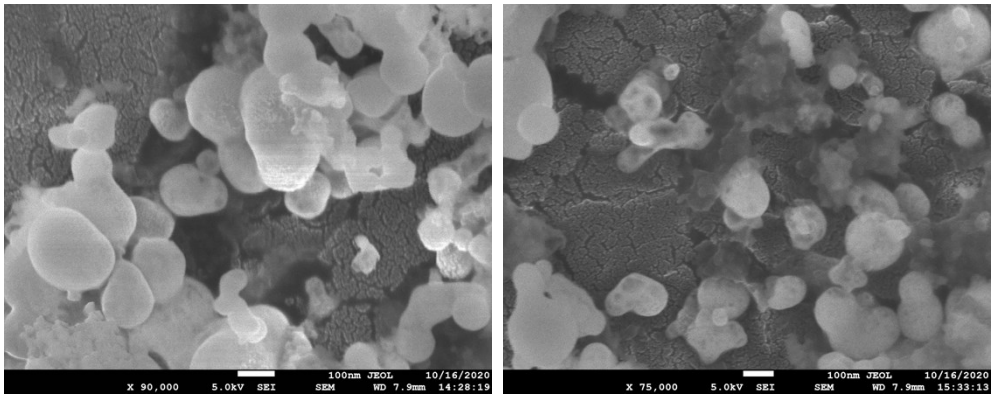

Figure S3: FE-SEM images of Hg adsorbed TTP-1

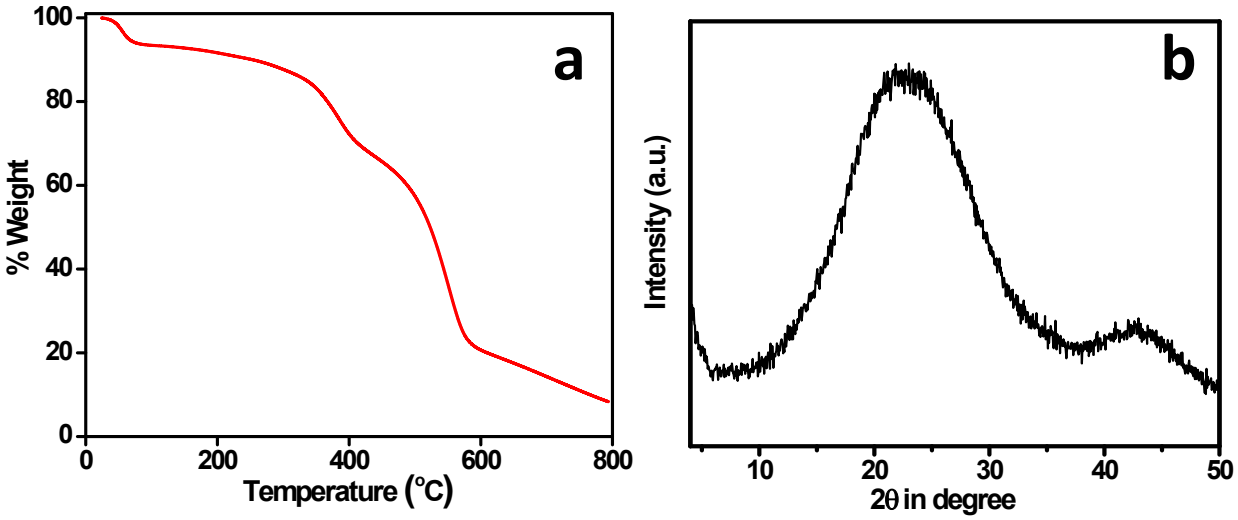

Figure S4: TGA profile (a) and PXRD pattern of TTP-1 (b).

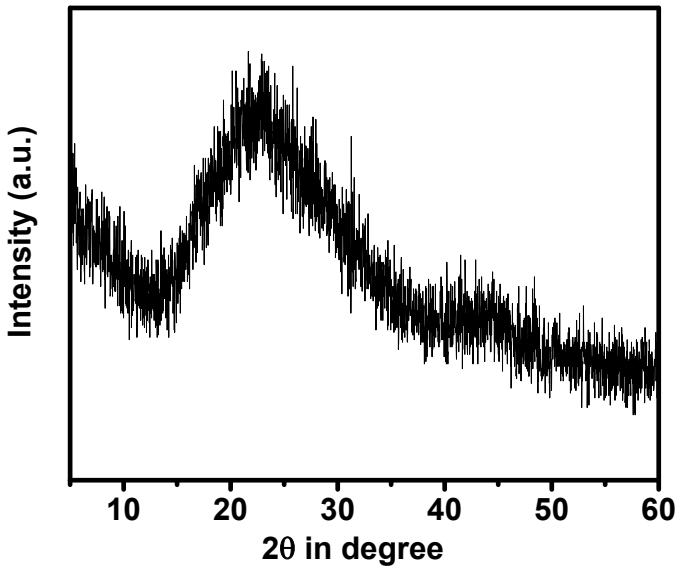

Figure S5: PXRD pattern of TTP-1 after recycling experiment.

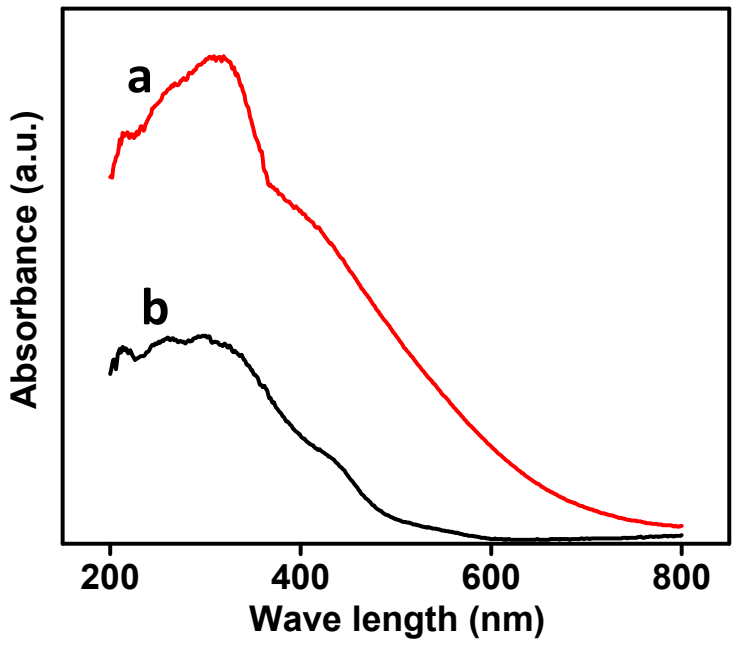

Figure S6: Solid state UV-Vis absorption spectra of TTP-1 before (a) and after (b) Hg capture**.**

Table S1: Selectivity in the adsorption over TTP-1 using 100:1 metal ion composition

	Metal ion	Concentration	
		Initial concentration (mg/L)	Final concentration (mg/L)
1.	Na(I)	112	91
2.	Mg(II)	98	76
3.	Zn(II)	102	62
4.	Co(II)	97	58
5.	Hg(II)	1	0.0011
6.	Cd(II)	1	0.0013
7.	Pb(II)	1	0.0019

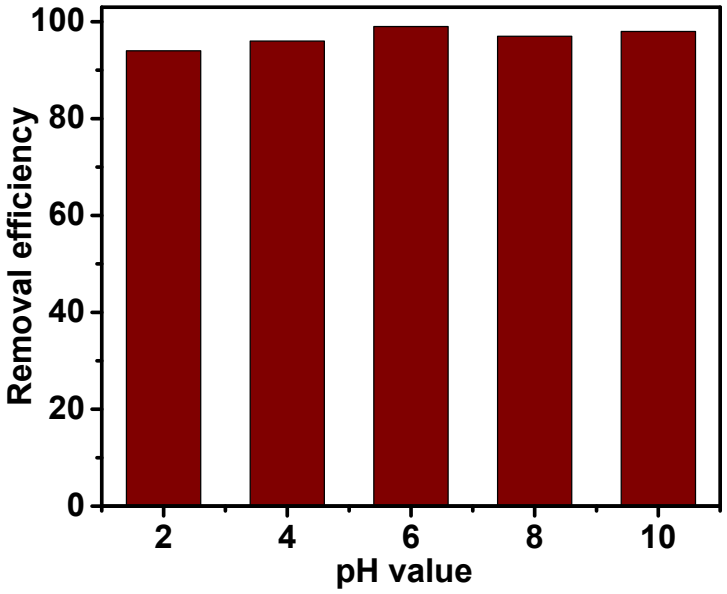

Figure S7: Hg(II) Removal efficiency of TTP-1 at different pHs.

Methodology

The complex of the ligand with a different number of Hg^{2+} ions was optimized using Gaussian 16 suites of the program.[1] The ab-initio quantum chemical calculation coupled with atoms in molecules (AIM) analysis illustrates noncovalent interactions.[1-8] In this study, we have applied B3LYP density functional coupled with 6-31+G(d) basis set for C, H, N, and S whereas LanL2DZ basis function and effective core potential for the heavy Hg^{2+} which known to produce a reliable result. During optimization, we have employed the frozen core approximation and tight convergence criterion. Harmonic frequency calculations were performed to ensure that all the structures are at local minima. The stabilization energy for the complexes was calculated based on the following equation

$$\Delta E_{Stab} = E_{Comp} - E_{Hg^{2+}} - E_{Lig} \qquad \text{* MERGEFORMAT (1.1)}$$

Where, E_{Comp}, $E_{Hg^{2+}}$, and E_{Lig} are zero-point vibrational energy (ZPVE) corrected energies of the complex, the Hg^{2+}, and the ligand.

To evaluate the nature of noncovalent interactions, AIM analysis was performed to generate a molecular density map using Atoms in Molecules (AIM) software.[3, 9-17] Further, electron density (ρ) and Laplacian of electron density ($\nabla^2\rho$, L) and bond ellipticity were calculated at each bond critical point (BCPs) to reveal the nature of the interaction between two atoms. It is important to note that only those BCPs were considered whose ρ and L are higher than 0.002 and 0.02 a. u., respectively, which are considered the threshold for noncovalent interaction. The bond ellipticity can be written as follows

$$\varepsilon = \frac{\lambda_1}{\lambda_2} - 1 \qquad \text{* MERGEFORMAT (1.2)}$$

Where, λ's are the negative vectors associated with the hessian of ρ at that BCP and $\lambda_2 \leq \lambda_1$.

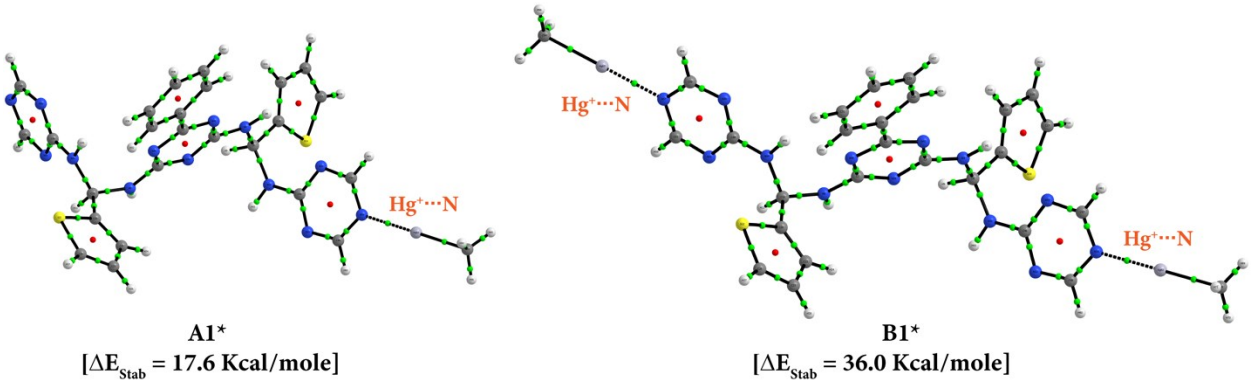

Figure S8: Molecular density map of the most stable conformation of (a) 1:1 complex (A1*) and (b) 1:2 complex (B1*) between the model monomer and CH_3Hg^+ generated from the wavefunction calculated from of the optimized geometry at B3LYP density functional method using 6-31+G(d) basis set for C, H, N, and S and LanL2DZ basis set with effective core potential for Hg^+. The green spheres indicate the bond critical point (BCP), and the red spheres represent the ring critical point (RCP). The spheres in white, grey, yellow, blue, and light grey represent H,

References

1. M. J. Frisch, G. W. T., H. B. Schlegel, G. E. Scuseria, M. A. Robb, J. R. Cheeseman, G. Scalmani, V. Barone, G. A. Petersson, H. Nakatsuji, X. Li, M. Caricato, A. V. Marenich, J. Bloino, B. G. Janesko, R. Gomperts, B. Mennucci, H. P. Hratchian, J. V. Ortiz, A. F. Izmaylov, J. L. Sonnenberg, D. Williams Young, ; F. Ding, F. L., F. Egidi, J. Goings, B. Peng, A. Petrone, T. Henderson, D. Ranasinghe, V. G. Zakrzewski, J. Gao, N. Rega, G. Zheng, W. Liang, M. Hada, M. Ehara, K. Toyota, R. Fukuda, J. Hasegawa, M. Ishida, T. Nakajima, Y. Honda, O. Kitao, H. Nakai, T. Vreven, K. Throssell, J. A. Montgomery, Jr., J. E. Peralta, F. Ogliaro, M. J. Bearpark, J. J. Heyd, E. N. Brothers, K. N. Kudin, V. N. Staroverov, T. A. Keith, R. Kobayashi, J. Normand, K. Raghavachari, A. P. Rendell, J. C. Burant, S. S. Iyengar, J. Tomasi, M. Cossi, J. M. Millam, M. Klene, C. Adamo, R. Cammi, J. W. Ochterski, R. L. Martin, K. Morokuma, O. Farkas, J. B. Foresman, and D. J. Fox, Gaussian 16, Revision A.03. *Gaussian, Inc., Wallingford CT* **2016**.
2. K. Yamanou, Y. Tatamitani, and T. Ogata, *J. Phys. Chem. A* 2009**, 113** (15), 3476-3480.
3. R. F. W. Bader, *Chem. Eur. J.* 2006, **12** (30), 7769-7772.
4. M. Solimannejad, and L. Pejov, *J. Phys. Chem. A* 2005**, 109** (5), 825-831.
5. Y. Bu, and Z. Cao, *J. Phys. Chem. B* 2002**, 106** (7), 1613-1621.
6. T. A. Wesolowski, O. Parisel, Y. Ellinger, and J. Weber, *J. Phys. Chem. A* 1997**, 101** (42), 7818-7825.
7. A. Nowek, and J. Leszczyński, *J. Phys. Chem. A* 1997**, 101** (20), 3784-3788.
8. J. C. Ching, and E. O. Schlemper, *Inorg. Chem.* 1975**, 14** (10), 2470-2474
9. R. W. Bader, and C. Matta, *Found Chem* 2013**, 15** (3), 253-276.
10. R. F. W. Bader, *Comp. Theor. Chem.* 2010, **943** (1–3), 2-18.
11. R. F. W. Bader, *J. Phys. Chem. A* 2009**, 113** (38), 10391-10396.
12. C. F. Matta, and R. F. W. Bader, *J. Phys. Chem. A* 2006**, 110** (19), 6365-6371.
13. R. F. W. Bader, *Chem. Phys. Lett.* 2006**, 426** (1–3), 226-228.
14. F. Cortés-Guzmán, Bader, and R. F. W. Bader, *Coord. Chem. Rev.* 2005**, *249*** (5–6), 633-662.
15. R. F. W. Bader, R. J. Gillespie, and F. Martín, *Chem. Phys. Lett.* 1998**, 290** (4–6), 488-494.
16. R. G. A. Bone, and R. F. W. Bader, *J. Phys. Chem.* 1996**, 100** (26), 10892-10911.
17. R. F. W. Bader, *Acc. Chem. Res.* 1975, **8** (1), 34-40.